Downregulated ALKBH5 contributes to myocardial ischemia/reperfusion injury by increasing m^{6}A modification of Trio mRNA

Jiaxin Li[1,2#^], Jieshan Chen[3#], Mingyi Zhao[4#], Zhetao Li[1,5], Nanbo Liu[5], Heng Fang[1,6], Miaoxian Fang[2], Ping Zhu[1,4], Liming Lei[2*], Chunbo Chen[1,2,6,7*^]

[1]The Second School of Clinical Medicine, Southern Medical University, Guangzhou, China; [2]Department of Intensive Care Unit of Cardiac Surgery, Guangdong Cardiovascular Institute, Guangdong Provincial People's Hospital, Guangdong Academy of Medical Sciences, Guangzhou, China; [3]Department of Emergency, Maoming People's Hospital, Maoming, China; [4]Department of Cardiac Surgery, Guangdong Cardiovascular Institute, Guangdong Provincial People's Hospital, Guangdong Academy of Medical Sciences, Guangzhou, China; [5]Department of Medical Sciences, Guangdong Provincial People's Hospital, Guangdong Academy of Medical Sciences, Guangzhou, China; [6]Department of Critical Care Medicine, Guangdong Provincial People's Hospital, Guangdong Academy of Medical Sciences, Guangzhou, China; [7]Department of Critical Care Medicine, Maoming People's Hospital, Maoming, China

Contributions: (I) Conception and design: C Chen, L Lei; (II) Administrative support: J Chen, P Zhu; (III) Provision of study materials or patients: M Zhao, Z Li; (IV) Collection and assembly of data: J Li, H Fang, M Fang; (V) Data analysis and interpretation: J Li, N Liu; (VI) Manuscript writing: All authors; (VII) Final approval of manuscript: All authors.

[#]These authors contributed equally to this work.

[*]These authors contributed equally to this work.

Correspondence to: Chunbo Chen. The Second School of Clinical Medicine, Southern Medical University, 253 Middle Industrial Avenue, Guangzhou 510282, China. Email: gghccm@163.com; Liming Lei. Department of Intensive Care Unit of Cardiac Surgery, Guangdong Cardiovascular Institute, Guangdong Provincial People's Hospital, Guangdong Academy of Medical Sciences, 106 Zhongshan 2nd Road, Guangzhou 510100, China. Email: anesthlei@sina.com.

Background: The modification of N^6-methyladenosine (m^{6}A) is a dynamic and reversible course that might play a role in cardiovascular disease. However, the mechanisms of m^{6}A modification in myocardial ischemia/reperfusion injury (MIRI) remain unclear.

Methods: A mouse model of MIRI and a cell model of oxygen-glucose deprivation/reperfusion (OGD/R) HL-1 cells were employed. In an *in vivo* study, the total RNA m^{6}A modification levels were determined by dot blot, and the key genes related to m^{6}A modification were screened by real-time quantitative polymerase chain reaction (RT-qPCR) and Western blot. In an *in vitro* study, the effects of AlkB homolog 5 (ALKBH5), an RNA demethylase, on cell proliferation, cell injury, and apoptosis were detected by the 3-(4,5-dimethylthiazol-2-yl)-5-(3-carboxymethoxyphenyl)-2-(4-sulfophenyl)-2H-tetrazolium (MTS) assay, lactate dehydrogenase (LDH) and cardiac troponin-I (cTnI) levels, and flow cytometry. Besides, the m^{6}A modification-changed and differentially expressed messenger RNA (mRNA) were determined by methylated RNA immunoprecipitation sequencing (MeRIP-seq) and RNA sequencing (RNA-seq) in *ALKBH5*-overexpressed HL-1 cells. Finally, the mRNA levels of the promising targeted gene were examined by RT-qPCR and its m^{6}A modification levels were examined by MeRIP-qPCR.

Results: Our results showed that RNA m^{6}A modification was involved in MIRI, in which *ALKBH5* was downregulated. Functionally, by overexpressing or silencing ALKBH5 in experimental cells, we verified its protective properties on cell proliferation, cell injury, and apoptosis in the process of MIRI. Besides, we provided a mass of latent different mRNAs with m^{6}A modification variation in ALKBH5-overexpressed HL-1 cells. Mechanistically, we further screened the most potential targeted mRNAs and suggested that triple functional domain (Trio) mRNA could be upregulated by ALKBH5 by reducing m^{6}A level of Trio.

^ ORCID: Jiaxin Li, 0000-0002-6542-8855; Chunbo Chen, 0000-0001-5662-497X.

Conclusions: This study demonstrated that the downregulated *ALKBH5* might contribute to MIRI process by increasing the m^{6}A modification of Trio mRNA and downregulating Trio.

Keywords: AlkB homolog 5 (ALKBH5); N^6-methyladenosine modification (m^{6}A modification); myocardial ischemia/reperfusion injury (MIRI)

Submitted Feb 15, 2022. Accepted for publication Mar 23, 2022.
doi: 10.21037/atm-22-1289
View this article at: https://dx.doi.org/10.21037/atm-22-1289

Introduction

Acute myocardial infarction is one of the major reasons for death in cardiovascular disease patients, usually caused by sudden occlusion of the coronary artery (1). The main remedy for acute myocardial infarction is myocardial reperfusion. However, this approach can induce myocardial ischemia/reperfusion injury (MIRI) (2) and might lead to severe arrhythmia and in-hospital death (3). At a tertiary hospital, the mortality of patients with veno-arterial extracorporeal membrane oxygenation after the refractory cardiogenic shock was shown to be around 58% (4). In the complex pathologic process of MIRI, various stages are involved, involving platelet activation, oxidative stress, endothelial dysfunction, and inflammatory response (5). Therapeutic strategies for MIRI mainly consist of non-pharmacological interventions (ischemic preconditioning, ischemic postconditioning, and remote ischemic preconditioning), pharmacological interventions (cyclosporine A, atrial natriuretic peptide, and glucagon-like peptide 1) (6,7), and even implementation of human-induced pluripotent cells (8). Although cell and animal experiments have confirmed the effectiveness of the therapies, the results of clinical trials have been disappointing. A single cardiac protection strategy is not effective in improving MIRI, but the combination of multiple protection strategies or collaborative multi-target therapies is promising for MIRI therapy. Therefore, it is imperative to further study the molecular mechanism of MIRI and provide a basis for exploring more therapeutic targets.

Epigenetics is a key component of genetics, encompassing RNA methylation, DNA methylation, histone, and non-coding RNA modification (9,10). The N^6-methyladenosine (m^{6}A) is a methylated modification at the adenine N^6 position (11). Modification of m^{6}A is a dynamic and reversible course regulated by methylase, demethylase, and binding proteins (12). Proteins related to m^{6}A modification are divided into 3 categories, namely writer (writing protein), reader (reading protein), and eraser (erasing protein). Among them, writing proteins [methyltransferases such as methyltransferase-like (METTL)3, METTL4, METTL14, Wilms tumor 1-associated protein (WTAP)] are mainly responsible for adding m^{6}A modification to RNA (13,14). Erasing proteins [demethylases such as fat mass and obesity-associated (FTO) and AlkB homolog 5 (ALKBH5)] are mainly responsible for removing m^{6}A modification from RNA (15,16). Reading protein is mainly responsible for making m^{6}A modification function.

We know that m^{6}A can affect all phases of the messenger RNA (mRNA) life cycle, such as splicing, nuclear export, stability, translation, and degradation (17). In recent years, it has been revealed that continuous dynamic regulation of m^{6}A is crucial in cardiovascular diseases including atherosclerosis, MIRI, myocardial hypertrophy, and heart failure (18-20). Myocardial injury could be caused by inflammation, oxidative stress, and metabolic disorder of energy, which occurs during ischemia-reperfusion (21). These pathological stimuli might relate to the methylation of m^{6}A RNA (22). As a methyltransferase, METTL3 can selectively bind to RNA with m^{6}A, which can further impress subsequent metabolic levels by regulating mRNA stability (23). A study showed that METTL3 can accelerate the development of acute ischemic stroke by mediating m^{6}A methylation (22). Interestingly, growing m^{6}A methylation could be mediated by increased METTL3 or decreased ALKBH5 to result in autophagy in hypoxic/reoxygenated cardiomyocytes and ischemia-reperfusion mice hearts (24). These findings suggest that the upregulation of m^{6}A modification may aggravate the injury in ischemic and hypoxic conditions in different organs. In a recent study, forced expression of ALKBH5 markedly reduced the cardiac infarct size, suggesting its therapeutic potential in heart regeneration during postnatal and adult injury (25). Therefore, we were inspired to focus on the independent effect of ALKBH5 on alleviating MIRI and its underlying

mechanisms. However, studies on the involvement of ALKBH5 in MIRI have been rarely reported.

Triple functional domain (Trio), a Rho guanine nucleotide exchange factor, has been shown to be related to cytoskeleton dynamics and actin remodeling, and plays various roles in cell migration and cytoskeleton reorganization (26).

In this study, we identified the elevated m^6A level in total RNA in the MIRI mice. Functionally, we determined the influences of ALKBH5 overexpression on the proliferation, cell injury, apoptosis, and m^6A level in the oxygen-glucose deprivation/reperfusion (OGD/R)-induced HL-1 cells and the impacts of ALKBH5 silencing on these functions. We further filtered and analyzed the differentially expressed mRNAs related to m^6A methylation change in ALKBH5-overexpressed HL-1 cells through methylated RNA immunoprecipitation sequencing (MeRIP-seq, also known as m^6A-IP-Seq) and RNA sequencing (RNA-seq). Taken together, our study might provide some potential molecular targets (mRNAs), which are mediated by ALKBH5 and connected with m^6A modification in MIRI. We present the following article in accordance with the ARRIVE reporting checklist (available at https://atm.amegroups.com/article/view/10.21037/atm-22-1289/rc).

Methods

Animals

Specific pathogen-free C57BL/6 mice (male, 6–7 weeks old, weighing 16–18 g) were purchased from Guangdong Medical Experimental Animal Center (Guangzhou, China). The breeding environment was 20–25 ℃, 50–60% humidity, alternating day and night, and feeding and drinking alone. Our study was approved by the Ethics Committee of Guangdong Provincial People's Hospital (No. KY-D-2021-102-01) and conducted with the NIH guiding principles for the care and use of animals. A protocol was prepared before the study without registration.

Establishment of MIRI mouse model

A total of 18 mice were randomly divided into 2 groups, a sham group (n=9), and a MIRI group (n=9). Operators were blinded to the allocation. The MIRI mice were established by ligation of the left anterior descending coronary artery (27). After peritoneal anesthesia with 1% pentobarbital sodium, surgical incisions were made between the third and fourth sternal intercostals to expose the heart. The left anterior descending coronary artery was identified under the microscope, and the left atrial appendage was ligated at the 1 cm lower margin with a suture needle to induce ischemia for 30 minutes. Then, the slip knot was unwound for 24 h of reperfusion. The sham group was not ligated. No unexpected adverse events were observed and animals were not excluded. Myocardium and peripheral blood were collected after the mice were sacrificed at 24 h reperfusion. Each group was analyzed in at least 3 independent experiments, which made the group size of each experiment 3. Some myocardial tissue was preserved with liquid nitrogen to prevent RNA degradation, while the rest was fixed with 4% paraformaldehyde or performed 2,3,5-triphenyltetrazolium chloride (TTC) staining experiments. After centrifugation, the serum was collected and stored at 4 ℃.

Detection of lactate dehydrogenase (LDH) and cardiac troponin-I (cTnI) in the serum

LDH and cTnI concentrations in serum were sent to KingMed Diagnostics Group Co., Ltd. (Guangzhou, China) for biochemical testing.

TTC staining

The mice were euthanized by cervical dislocation, the chest was opened, and the heart was exposed and removed. Then the heart was frozen at –80 ℃ for 30 minutes and then sliced into 1-mm thick sections. Next, the heart sections were placed in 2% TTC (Sigma Aldrich, St. Louis, MO, USA) and incubated at 37 ℃ for 15 minutes. After fixation with 10% paraformaldehyde, the sections were photographed. Red indicated living tissue and white was infarcted tissue.

Terminal deoxynucleotidyl transferase deoxyuridine triphosphate (dUTP) nick end labeling (TUNEL) staining

The myocardial tissues in sham and MIRI groups were fixed, dehydrated, paraffin-embedded, and cut into 5-μm slices. Subsequently, the slices were dewaxed to water, addressed with protease K (Roche, Basel, Switzerland) for 10 minutes, and TUNEL mixture (Roche) at 37 ℃ for 1 h. After the reaction was terminated, the slices underwent a series of treatments, including 4',6-diamidino-2-phenylindole (DAPI) coloration for 10 minutes, washing, and sealing. The TUNEL staining was observed under a microscope (Olympus, Tokyo, Japan).

m^{6}A dot blot

Total RNA was mixed with the incubation buffer (3 times volume) and denatured at 65 ℃ for 5 minutes. The samples (125 or 250 ng) in saline-sodium citrate (SSC) buffer (Sigma-Aldrich, Saint Louis, MO, USA) were transferred to Amersham Hybond-N$^+$ membrane (GE Healthcare, Chicago, IL, USA) on Bio-Dot Apparatus (Bio-Rad, Hercules, CA, USA). After crosslinking for 5 minutes, the sample was stained with 0.02% methylene blue (Sangon Biotech, Shanghai, China). After the blue dots were scanned, the samples were exposed to anti-m^{6}A (Synaptic System) at 4 ℃ overnight, followed by secondary antibodies. Dot blots were displayed with an imaging system.

Establishment of OGD/R HL-1 cells

The HL-1 cells (Sigma-Aldrich, USA) were grown in Claycomb medium (Sigma-Aldrich, USA) with 10% fetal bovine serum (FBS) (Gibco, catalog No. 10099141; Amarillo, TX, USA), 100 μmol/mL penicillin/streptomycin at 37 ℃ with 5% CO_2. For OGD/R, HL-1 cells were hatched with Dulbecco's modified Eagle medium (DMEM) without sugar and FBS in the incubator (94% N_2, 5% CO_2, and 1% O_2) at 37 ℃ for 6 h. Then, HL-1 cells were grown with the complete medium at 37 ℃ and 5% CO_2 for another 48 or 72 h.

Cell transfection

Empty vector (LV003) and ALKBH5 overexpression plasmid were gained from General Biol (Anhui, China). Negative control small interfering RNAs (siRNAs, si-NC) and ALKBH5 siRNAs (si-ALKBH5-1, si-ALKBH5-2, and si-ALKBH5-3) were acquired from Gene Pharma (Shanghai, China). The sequence of si-ALKBH5-1 was 5'-TCGTGTCCGTGTCTTTCTT-3'; the sequence of si-ALKBH5-2 was 5'- GCTGCAAGTTCCAGTTCAA-3'; and the sequence of si-ALKBH5-3 was 5'-GACTGTGCTCAGTGGGTAT-3'. The OGD/R HL-1 or HL-1 cells were transfected with the plasmids (LV003 or ALKBH5 overexpression plasmid) or oligonucleotides (NC siRNA or si-ALKBH5) using Lipofectamine 3000 (Invitrogen, Waltham, MA, USA) for 48 h.

Real-time quantitative polymerase chain reaction (RT-qPCR)

Total RNAs were harvested from the processed HL-1 cells or the ground myocardial tissue with TRIzol reagent (Invitrogen, USA). PrimeScript^{TM} RT reagent Kit (TaKaRa, Shiga, Japan) was utilized to synthesize complementary DNA (cDNA), and RNA acted as a template. Then, polymerase chain reaction (PCR) amplification was conducted with SYBR Green qPCR Master Mix (DBI Bioscience, Shanghai, China). The data was calculated through $2^{-\Delta\Delta Ct}$ method. Primer sequences are presented in *Table 1*.

Western blot

The processed HL-1 cells or myocardial tissue that had been ground were exposed to radioimmunoprecipitation assay (RIPA; Beyotime, Jiangsu, China) with protease inhibitors. Then, the protein in the loading was heated at 100 ℃ for denaturation after quantification. Proteins (40 μg) were separated by electrophoresis with sodium dodecyl sulfate polyacrylamide gel electrophoresis (SDS-PAGE) and transferred to the polyvinylidene fluoride (PVDF) membrane (Millipore, Burlington, MA, USA). Subsequently, the protein was sealed with 5% skim milk for 2 h and treated with anti-ALKBH5 (Proteintech, catalog No. 16837-1-AP; Rosemont, IL, USA), anti-YTHDF2 (Proteintech, catalog No. 24744-1-AP), and anti-GAPDH (Proteintech, catalog No. 60004-1-lg) at 4 ℃ overnight, and secondary antibodies for 1 h. Finally, the blotting of protein was developed after treatment with an enhanced chemiluminescence (ECL) kit (Thermo Fisher Scientific, Waltham, MA, USA).

Cell proliferation assay

Cell proliferation was examined by 3-(4,5-dimethylthiazol-2-yl)-5-(3-carboxymethoxyphenyl)-2-(4-sulfophenyl)-2H-tetrazolium (MTS) assay. The HL-1 cells were harvested and counted (2.5×10^4/mL), then inoculated with 200 μL/well into 96-well plates, and cultured for 24 h. After different treatments, each well was supplemented with 100 μL MTS solution, which was cultured for 3 h at 37 ℃. The absorbance was tested at 490 nm with a microplate reader.

Enzyme-linked immunosorbent assay (ELISA)

In line with the instructions, the content of LDH was tested using an LDH Cytotoxicity Assay Kit (Beyotime, catalog No. C0016; China).

Table 1 Primer sequences in RT-qPCR experiments

Primer	Sequence (5'–3')	Product length (bp)
M-*Fto*-F	GAGCAGCCTACAACGTGACT	200
M-*Fto*-R	GAAGCTGGACTCGTCCTCAC	
M-*ALKBH5*-F	TGCTGCGTATGGGGCTTAAA	182
M-*ALKBH5*-R	ATGCCTAACAGGAGCAACCC	
M-*YTHDF2*-F	CAGGCAAGGCCGAATAATGC	167
M-*YTHDF2*-R	TCTCCGTTGCTCAGTTGTCC	
M-*Mettl3*-F	ATCTTGGCTCTATCCGGCTG	147
M-*Mettl3*-R	GATAGAGCTCCACGTGTCCG	
M-*Mettl14*-F	CTCCAGGTCGGAGTGTGAAC	102
M-*Mettl14*-R	AACCGTTTAAACCAGCCCCT	
M-*Neil3*-F	AGCCAGATTGCCATAGAACCC	234
M-*Neil3*-R	CCGGCCTTTTTCACCTCACA	
M-*Pnp*-F	GAGTGAGAGTGAGAAGAGCCAC	214
M-*Pnp*-R	CCTTTCCAATGTCTGTGCAGC	
M-*Trio*-F	CACTACTCCTCAAGACGGCA	247
M-*Trio*-R	CACAAGCACAAGAAGAGCCG	
M-*Zfp235*-F	CCAGCAGTGGTGACTGTGAT	91
M-*Zfp235*-R	TTGCACTGGTAGGCCTTCTG	
M-*Hexim2*-F	TCTGAGGCCTATGAGCGGTA	250
M-*Hexim2*-F	CCTCTCGGTTCCACATCTCG	
M-*Zfp81*-F	GCCCATGAGAATCCTCCCAA	220
M-*Zfp81*-R	CTCCACACTGCTTACACACA	
M-*Cuedc1*-F	CGGAACCAGTGAAACCAACC	244
M-*Cuedc1*-R	GTCTTCCTCTGCCTCACCGTA	
M-*Slc25a53*-F	GCATTCAGCTCTGCTCCCAT	242
M-*Slc25a53*-R	AGTGGCCAGAGCAGGACTTA	
M-*Msantd3*-F	CTGCCGGAGCAACTGTACTT	175
M-*Msantd3*-R	AGCATGAAGGTTCGGGTTGT	
M-*Map1a*-F	GGCAGGATCCACAGCCTT	162
M-*Map1a*-R	TTGGCAGGGTCATTTCCACT	
M-*GAPDH*-F	AGGTCGGTGTGAACGGATTTG	129
M-*GAPDH*-R	TGTAGACCATGTAGTTGAGGTCA	

RT-qPCR, reverse transcription quantitative polymerase chain reaction; F, forward; R, reversed.

Flow cytometry

The processed HL-1 cells were harvested and adjusted to 1×10^6/mL. Then, the cells were processed using Annexin V FITC/PI apoptosis kit (BioLegend, San Diego, CA, USA). Flow cytometry was adopted to confirm the apoptosis rate.

MeRIP-seq

As described in previous research (28), for MeRIP-seq, the m^{6}A antibody was used for the RIP experiment, and the RNA obtained was sent to Novogene Co., Ltd. (Beijing, China) for library construction and sequencing.

RNA-seq

The RNA-seq was also conducted by Novogene Co., Ltd. (Beijing, China) with the Illumina Novaseq 6000 platform (Illumina, San Diego, CA, USA). Briefly, after total RNA was quality-controlled, a cDNA library was constructed using an RNA-seq sample preparation kit (Illumina, USA). The sequenced reads were compared to the reference genome, and the genes or transcripts were annotated and quantified. StringTie [2016] was applied to annotate and quantify the expression.

Gene Ontology (GO) and Kyoto Encyclopedia of Genes and Genomes (KEGG) analysis

Based on the literature (29), the GO database was applied to elucidate the hierarchical relationship between gene functions. The KEGG database was applied to classify, annotate, and enrich signal pathways of differential genes referring to the previous study (30).

MeRIP-qPCR

We applied Magna MeRIP™ m^{6}A Kit (Millipore, Darmstadt, Germany) to conduct MeRIP, which could be applied to analyze m^{6}A modifications on a single transcript. Total RNA (150 μg) was randomly segmented into small nucleotides, which then were immuno-precipitated by magnetic beads precoated with anti-m^{6}A (10 μg, Millipore) or anti-IgG (10 μg, Millipore). Next, the m^{6}A-modified RNA fragments were eluted. Finally, MeRIP-qPCR was proceeded with specific primers. The primer sequences are

Table 2 Primer sequences in MeRIP-qPCR experiments

Primer	Sequence (5'–3')	Product length (bp)
M-*Neil3*-F	AGCCAGATTGCCATAGAACCC	234
M-*Neil3*-R	CCGGCCTTTTTCACCTCACA	
M-*Pnp*-F	GAGTGAGAGTGAGAAGAGCCAC	214
M-*Pnp*-R	CCTTTCCAATGTCTGTGCAGC	
M-*Trio*-F	CACTACTCCTCAAGACGGCA	247
M-*Trio*-R	CACAAGCACAAGAAGAGCCG	
M-*GAPDH*-F	AGGTCGGTGTGAACGGATTTG	129
M-*GAPDH*-R	TGTAGACCATGTAGTTGAGGTCA	

MeRIP-qPCR, methylated RNA immunoprecipitation quantitative polymerase chain reaction; F, forward; R, reversed.

presented in *Table 2*.

Statistical analysis

Statistical analysis was conducted with the software SPSS 22.0 (IBM Corp., Armonk, NY, USA). Measurement data was displayed as mean ± standard deviation (SD). One-way analysis of variance (ANOVA) was utilized for comparison between multiple groups, Bonferroni corrected *t*-test was utilized for comparison between 2 groups. Statistical significance was considered when $P<0.05$.

Results

Establishment of the MIRI mouse models

Biochemical test results denoted that the concentration of LDH and cTnI was memorably aggrandized in the MIRI model group versus that in the sham group (*Figure 1A*). The TTC staining results showed that the infarct size was notably augmented in the MIRI mice versus the sham group (*Figure 1B*). Meanwhile, TUNEL staining results indicated that TUNEL-positive cells were markedly increased in the MIRI group versus that in the sham group (*Figure 1C*). These data indicated the successful establishment of the MIRI mouse models.

Screening of the key genes related to m^{6}A modification in MIRI mice

Considering the vital function of m^{6}A modification in MIRI (22), we first determined the level of m^{6}A through a dot blot. The data indicated that the m^{6}A level in total RNA was observably elevated in the MIRI group versus that in the sham group, indicating that m^{6}A modification was relevant to MIRI (*Figure 1D*). Besides, on account of the Gene Expression Omnibus (GEO) database (GSE35421), we screened the genes associated with m^{6}A modification including *FTO*, *ALKBH5*, *YTHDF2*, *METTL3*, and *METTL14*. The RT-qPCR data displayed that *ALKBH5* was prominently downregulated, while *YTHDF2* was notably upregulated in the MIRI group with respect to that in the sham group (*Figure 1E*). Based on the RT-qPCR data, *ALKBH5* and *YTHDF2* with aberrant expression were selected for Western blot detection to further verify the key genes. The results indicated that the protein expression of *ALKBH5* was dramatically downregulated whereas the expression of *YTHDF2* was not obvious in the MIRI group versus that in the sham group (*Figure 1F,1G*). Overall, we verified that the m^{6}A level of total RNA was increased during MIRI, and *ALKBH5* was selected for follow-up experiments.

ALKBH5 overexpression enhances proliferation, suppresses LDH content, apoptosis, and decreases m^{6}A level in OGD/R-induced HL-1 cells

Subsequently, we verified the possible function of ALKBH5 overexpression in the OGD/R-treated HL-1 cells. We first transfected ALKBH5-overexpressed plasmid into HL-1 cells. The results displayed that the level of ALKBH5 was memorably heightened in the ALKBH5 group relative to that in the LV003 group, revealing the successful overexpression of ALKBH5 in HL-1 cells through transfection (*Figure 2A,2B*). Besides, we discovered that ALKBH5 expression was notably lowered in the LV003 + OGD/R group versus that in the LV003 group, while the decrease of ALKBH5 expression also could be reversed by ALKBH5 overexpression in the OGD/R HL-1 cells (*Figure 2C,2D*). Functionally, MTS data indicated that OGD/R could cause a distinct suppression in the proliferation of HL-1 cells, while ALKBH5 overexpression could markedly encourage the proliferation in the OGD/R-induced HL-1 cells (*Figure 2E*). ELISA data showed that relative to the LV003 group, LDH content was observably increased in the OGD/R group, which also could be notably weakened by ALKBH5 overexpression (*Figure 2F*). Flow cytometry data revealed that OGD/R could result in a striking enhancement in the apoptosis of HL-1 cells, while ALKBH5 overexpression could prominently attenuate this

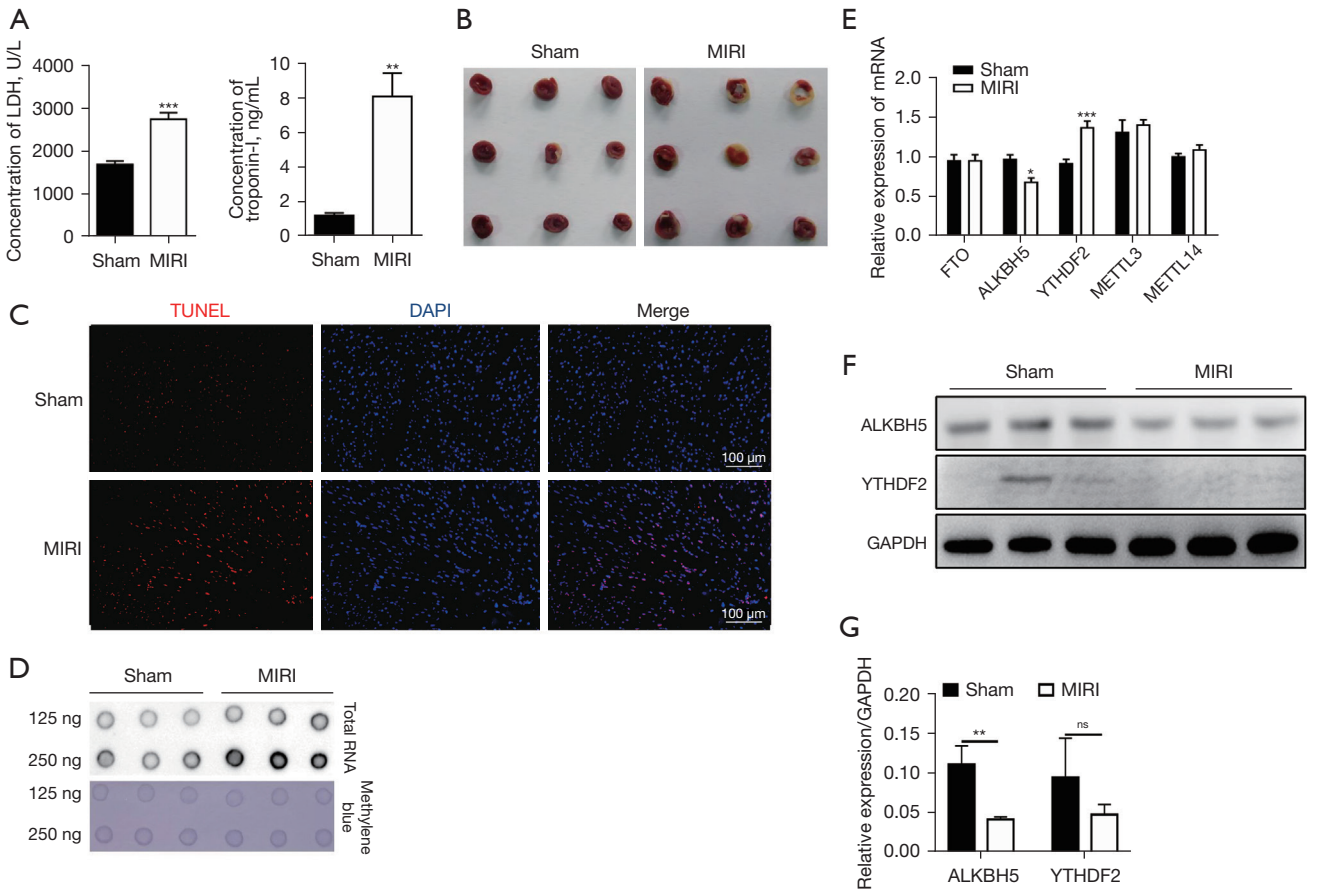

Figure 1 Establishment of MIRI mouse models and screening of the key genes related to m^{6}A modification. (A) LDH and cTnI concentrations in the serum of the sham and MIRI mice. (B) TTC staining in the myocardial tissues of the sham and MIRI mice. (C) TUNEL staining in the myocardial tissues of the sham and MIRI mice. Magnification, 100×. (D) m^{6}A dot blot in the sham and MIRI mice. And methylene blue staining (down) denoted input RNA, dot immunoblotting (up) denoted m6A modification. (E) RT-qPCR displayed the changes in *FTO*, *ALKBH5*, *YTHDF2*, *METTL3*, and *METTL14* expressions in sham (n=4) and MIRI mice (n=5). (F) Western blot analysis of ALKBH5 and YTHDF2 in sham and MIRI mice. (G) Relative quantification of ALKBH5 and YTHDF2 proteins. n=3 animals per group. *, P<0.05; **, P<0.01; ***, P<0.001. ns, not significance *vs.* the sham group; MIRI, myocardial ischemia/reperfusion injury; LDH, lactate dehydrogenase; cTnI, cardiac troponin-I; TTC, 2,3,5-triphenyltetrazolium chloride; TUNEL, terminal deoxynucleotidyl transferase deoxyuridine triphosphate nick end labeling; RT-qPCR, real-time quantitative polymerase chain reaction; FTO, fat mass and obesity-associated; ALKBH5, AlkB homolog 5; METTL, methyltransferase-like; m^{6}A, N^6-methyladenosine.

enhancement in the OGD/R HL-1 cells (*Figure 2G-2I*). Simultaneously, we also certified that the m^{6}A level of RNA could be dramatically increased in the LV003 + OGD/R group versus that in the LV003 group, while ALKBH5 overexpression could weaken this increase in the OGD/R HL-1 cells (*Figure 2J*). In general, these findings suggested that ALKBH5 overexpression had a protective role in cardiac OGD/R injury and reduced the m^{6}A level of total RNA.

ALKBH5 silencing reduces proliferation and heightens apoptosis and m^{6}A level in HL-1 cells

Conversely, we further investigated the impacts of

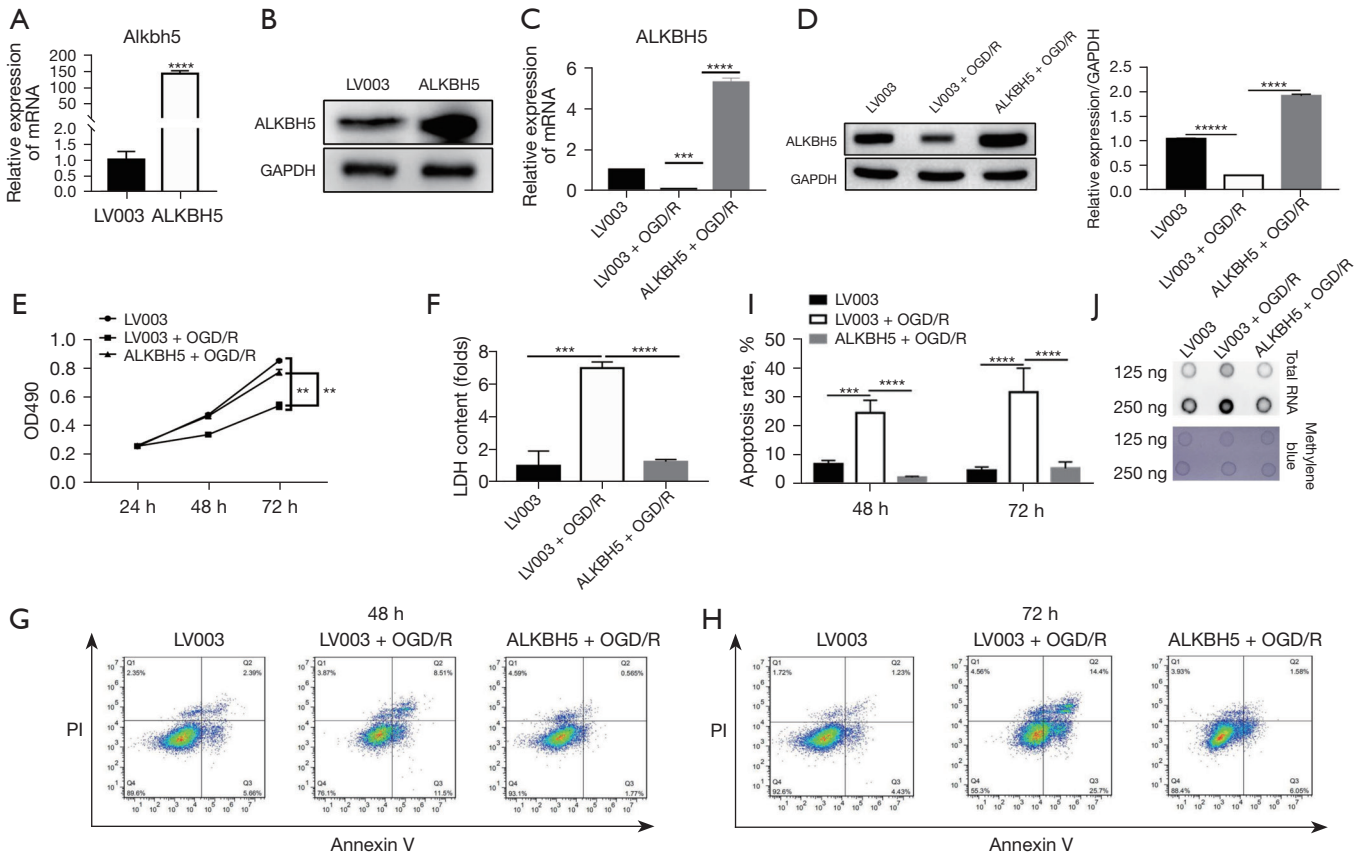

Figure 2 ALKBH5 overexpression enhanced proliferation, suppressed LDH content, apoptosis, and decreased m^{6}A level in the OGD/R-induced HL-1 cells. RT-qPCR (A) and Western blot (B) confirmed the overexpression effect of ALKBH5 in HL-1 cells. RT-qPCR (C) and Western blot (D) assessed ALKBH5 expression in the OGD/R-induced HL-1 cells after ALKBH5 overexpression (E) MTS showed the impact of ALKBH5 overexpression on cell proliferation. (F) ELISA assay evaluated the LDH content in the ALKBH5-overexpression OGD/R HL-1 cells. (G-I) Flow cytometry identified the changes of apoptosis in ALKBH5-overexpressed HL-1 cells under OGD/R at 48 and 72 h. (J) Dot blot examined the global m6A of RNA in the ALKBH5-overexpressed OGD/R HL-1 cells. **, P<0.01; ***, P<0.001; ****, P<0.0001; *****, P<0.00001. LDH, lactate dehydrogenase; OGD/R, oxygen glucose deprivation/reperfusion; RT-qPCR, reverse transcription polymerase chain reaction; ELISA, enzyme-linked immunosorbent assay; ALKBH5, AlkB homolog 5; m^{6}A, N^6-methyladenosine; MTS, 3-(4,5-dimethylthiazol-2-yl)-5-(3-carboxymethoxyphenyl)-2-(4-sulfophenyl)-2H-tetrazolium.

ALKBH5 silencing on the function and m^{6}A modification in HL-1 cells. We first transfected 3 ALKBH5 interference fragments into HL-1 cells, and the results manifested that ALKBH5 expression was markedly lower in ALKBH5 silencing groups versus that in the si-NC group, especially si-ALKBH5-2 (*Figure 3A*,*3B*). We chose si-ALKBH5-2 to silence ALKBH5 in HL-1 cells. Then, we testified that ALKBH5 silencing dramatically repressed the proliferation of HL-1 cells (*Figure 3C*). Silencing of ALKBH5 also markedly elevated LDH concentration in HL-1 cells (*Figure 3D*). Additionally, flow cytometry results indicated that ALKBH5 silencing facilitated the apoptosis of HL-1 cells (*Figure 3E*,*3F*). Meanwhile, ALKBH5 silencing also contributed to the increase of global m^{6}A levels in HL-1 cells (*Figure 3G*). Thus, our results uncovered that ALKBH5 silencing, contrary to ALKBH5 overexpression, can disrupt normal function and increase the m^{6}A levels in HL-1 cells.

Global distribution of altered m^{6}A peaks of m^{6}A-modified mRNAs in ALKBH5-overexpressed HL-1 cells

We further studied the underlying mRNAs related to m^{6}A methylation in ALKBH5-overexpressed HL-1 cells

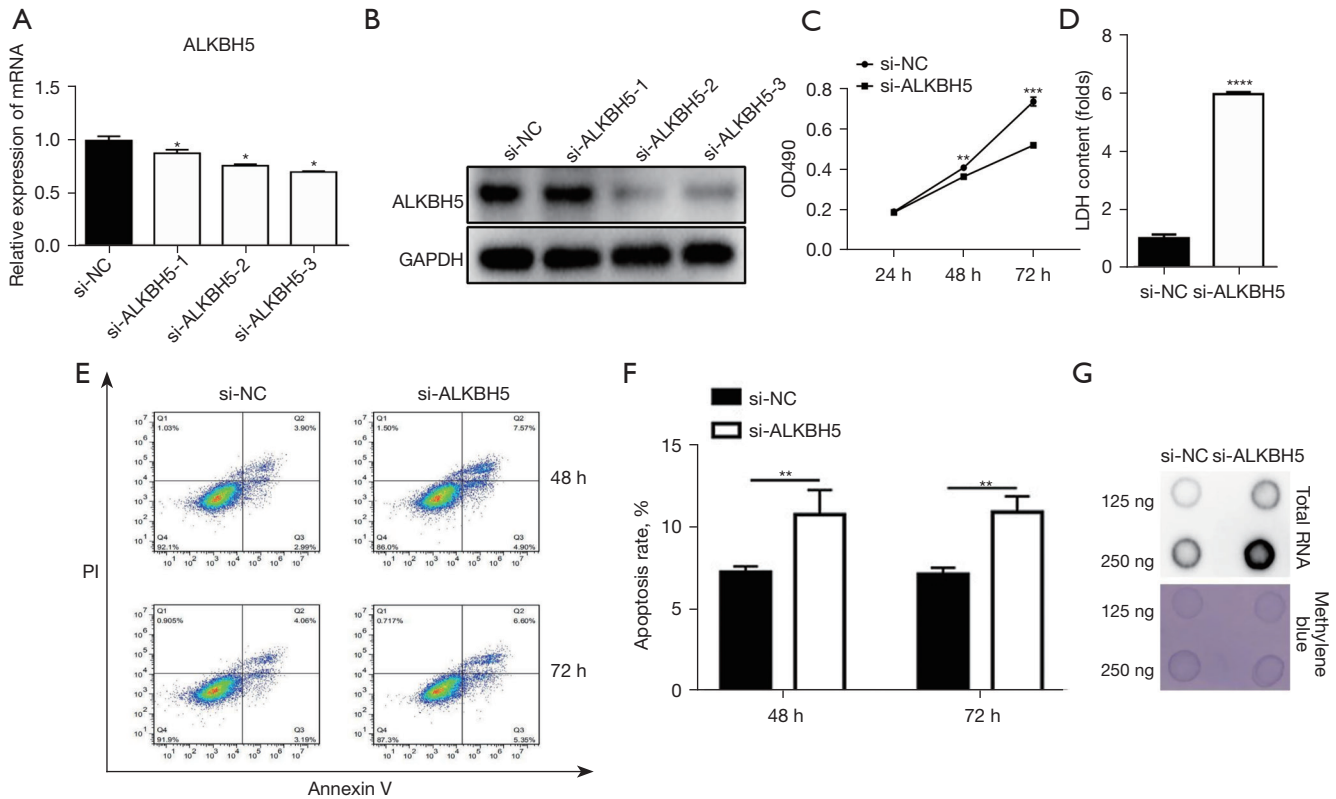

Figure 3 ALKBH5 silencing reduced proliferation and increased LDH content, apoptosis and m6A level in HL-1 cells. (A,B) RT-qPCR and Western blot showed ALKBH5 expression levels in HL-1 cells after transfection with si-ALKBH5-1, si-ALKBH5-2, and si-ALKBH5-3. (C) MTS displayed the changes in proliferation in ALKBH5-silenced HL-1 cells. (D) ELISA assay exhibited the change in LDH content. (E,F) Flow cytometry presented the changes in apoptosis. (G) Dot blot demonstrated the change in global m^{6}A level. *, P<0.05; **, P<0.01; ***, P<0.001; ****, P<0.0001. LDH, lactate dehydrogenase; RT-qPCR, reverse transcription polymerase chain reaction; ELISA, enzyme-linked immunosorbent assay; ALKBH5, AlkB homolog 5; m^{6}A, N^6-methyladenosine; MTS, 3-(4,5-dimethylthiazol-2-yl)-5-(3-carboxymethoxyphenyl)-2-(4-sulfophenyl)-2H-tetrazolium.

using m^{6}A-IP-Seq. Given the data analysis, we discovered a total of 503 m^{6}A peaks of m^{6}A-modified mRNAs had altered methylation levels, including 145 m^{6}A peaks with increased methylation levels (log10 likelihood ratio >2) and 358 m^{6}A peaks with decreased methylation levels (log10 likelihood ratio <–2). The changed m^{6}A peaks in LV003 and ALKBH5-transfected HL-1 cells were mainly distributed in the coding sequence (CDS) and 3'unstraslated regions (3'UTR) (*Figure 4A*,*4B*). Meanwhile, our data showed that 1 mRNA mainly had 1 altered m^{6}A peak with up-regulating or down-regulating (*Figure 4C*), and 1 gene mainly had 1 altered m^{6}A peak with up-regulating or down-regulating (*Figure 4D*). We also found that the upregulated m^{6}A peaks were mainly distributed on chromosomes 1, 2, and 6, and the downregulated m^{6}A peaks were mainly distributed on chromosomes 1, 2, and 9 (*Figure 4E*). To sum up, we screened out 503 altered m^{6}A peaks of m^{6}A-modified mRNAs changed in ALKBH5-overexpressed HL-1 cells and determined their basic distribution.

GO and KEGG analysis of mRNAs with upregulating and downregulating m^{6}A peaks in ALKBH5-overexpressed HL-1 cells

Subsequently, through MEME analysis (https://meme-suite.org/meme/), we confirmed the top 5 motifs of different m^{6}A peaks (*Figure 5A*). The data from GO analysis denoted that the mRNAs with upregulating and downregulating m^{6}A peaks were mainly enriched in the biological process (*Figure 5B*,*5C*). The KEGG analysis showed the disease-

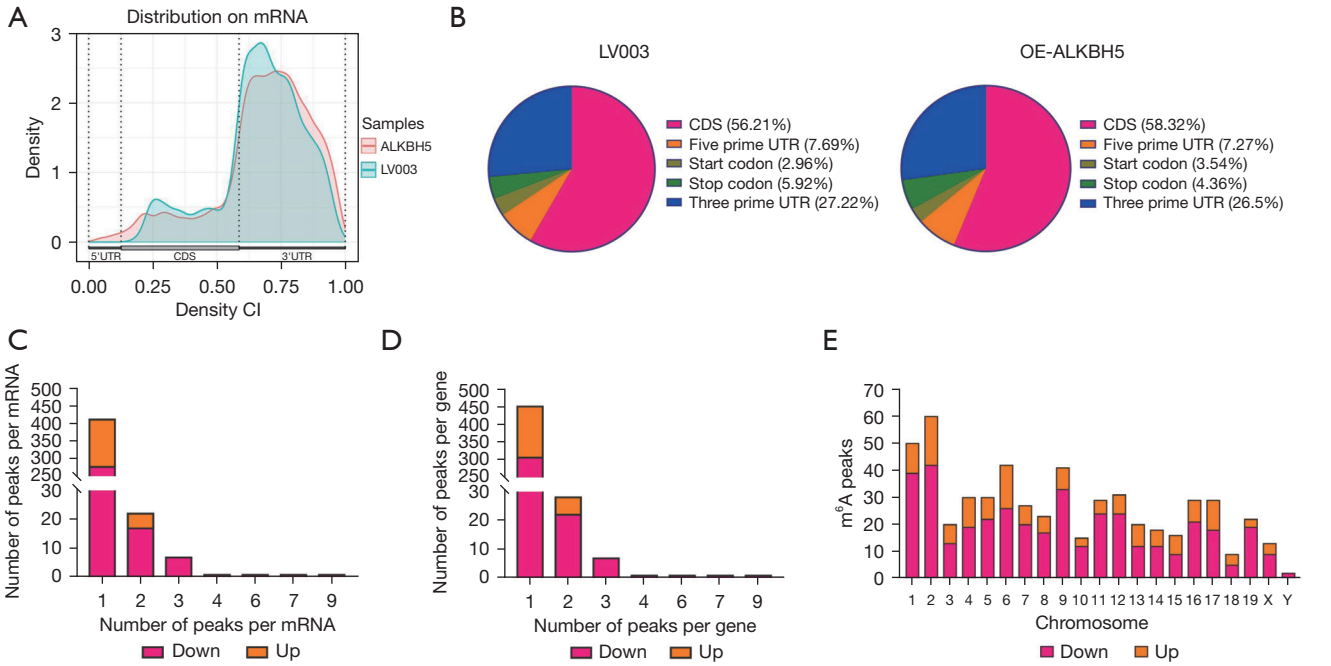

Figure 4 Global distribution of m^{6}A methylation-mediated peaks in ALKBH5-overexpressed HL-1 cells. Peaks with abnormal methylation modification were identified by MeRIP-Seq. (A) Distribution of peaks with different methylation modification. (B) The distribution of the changed peak in Mrna structural position. (C) The number of peaks changes per Mrna. (D) The number of peaks changes per gene. (E) The distribution of the altered m^{6}A peaks on each chromosome. mRNA, messenger RNA; CI, confidence interval; OE, overexpression; ALKBH5, AlkB homolog 5; m^{6}A, N^6-methyladenosine; CDS, coding sequence; UTR, untranslated region.

associated top 10 signaling in the enriched signaling pathways, most of which are associated with cell proliferation and apoptosis, including epidermal growth factor (ErbB), epidermal growth factor receptor (EGFR), mammalian target of rapamycin (mTOR), cyclic adenosine 3',5'-monophosphate (cAMP), pathways in cancer, forkhead box O (FoxO), and Ras-associated protein 1 (Rap1), and so on (*Figure 5D,5E*). Overall, we revealed that the mRNAs with upregulating and downregulating m^{6}A peaks were primarily relevant to proliferation and apoptosis, which might be regulated by 7 possible regulatory pathways.

Identification and analysis of mRNAs with different methylation modification and expression in ALKBH5-overexpressed HL-1 cells

On the basis of MeRIP-seq data, RNA-seq was adopted to determine the differently expressed mRNAs in ALKBH5-overexpressed HL-1 cells. We discovered 2,764 differentially expressed mRNAs, containing 1,280 upregulated mRNAs (logFC >1, P<0.05) and 1,484 downregulated mRNAs (logFC <–1, P<0.05) in ALKBH5-overexpressed HL-1 cells. Then, we visualized the distribution of the 2,764 different mRNAs using volcano plot and heat map (*Figure 6A,6B*). Besides, we analyzed the mRNAs with significant changes in both m^{6}A modification and mRNA expression, and the distribution was also displayed using 9 quadrantal diagrams. The data showed that there were 86 mRNAs with downregulated methylation modification and mRNA expression, 16 mRNAs with upregulated methylation modification and mRNA expression, 45 mRNAs with upregulated methylation modification, and downregulated mRNA expression, 44 mRNAs with downregulated methylation modification and upregulated mRNA expression (*Figure 6C*). The GO analysis revealed that these mRNAs mainly participated in the biological process (*Figure 6D*). The KEGG analysis showed that these mRNAs mainly involved pathways in cancer, insulin, ErbB, mitogen-activated protein kinase (MAPK) pathway, and so on (*Figure 6E*). Generally, we obtained vast mRNAs with different methylation modification and expression and enrichment potential pathways.

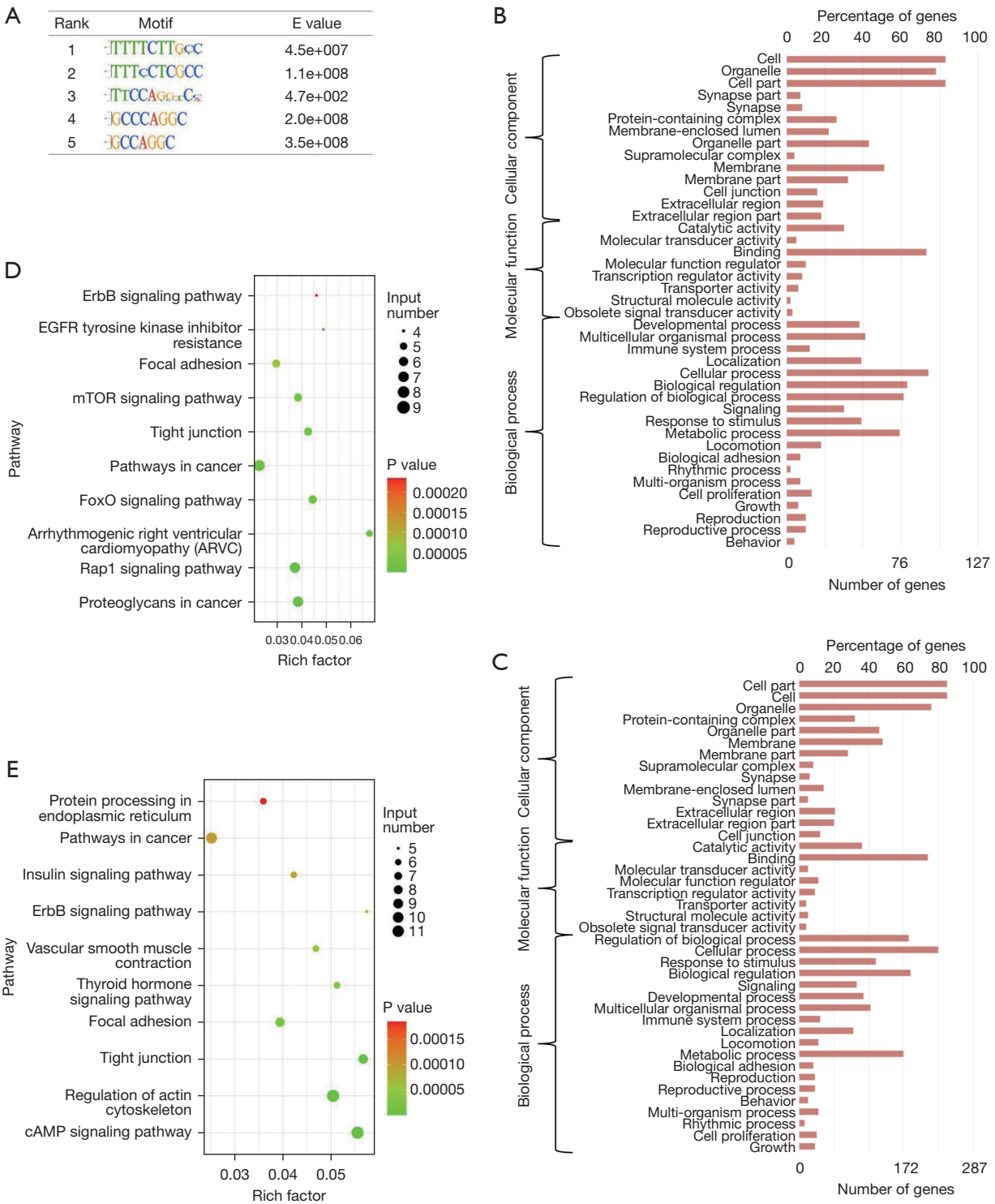

Figure 5 GO and KEGG analysis of mRNAs with upregulating and downregulating m^{6}A peaks in ALKBH5-overexpressed HL-1 cells. (A) Top 5 motifs of the different m^{6}A peaks were presented through MEME analysis. (B) GO analysis of the upregulated m^{6}A peaks. (C) GO analysis of the downregulated m^{6}A peaks. (D) KEGG analysis of the upregulated m^{6}A peaks. (E) KEGG analysis of the downregulated m^{6}A peaks. GO, Gene Ontology; KEGG, Kyoto Encyclopedia of Genes and Genomes; ALKBH5, AlkB homolog 5; m^{6}A, N^6-methyladenosine; ErbB, epidermal growth factor; EGFR, epidermal growth factor receptor; mTOR, mammalian target of rapamycin; FoxO, forkhead box O.

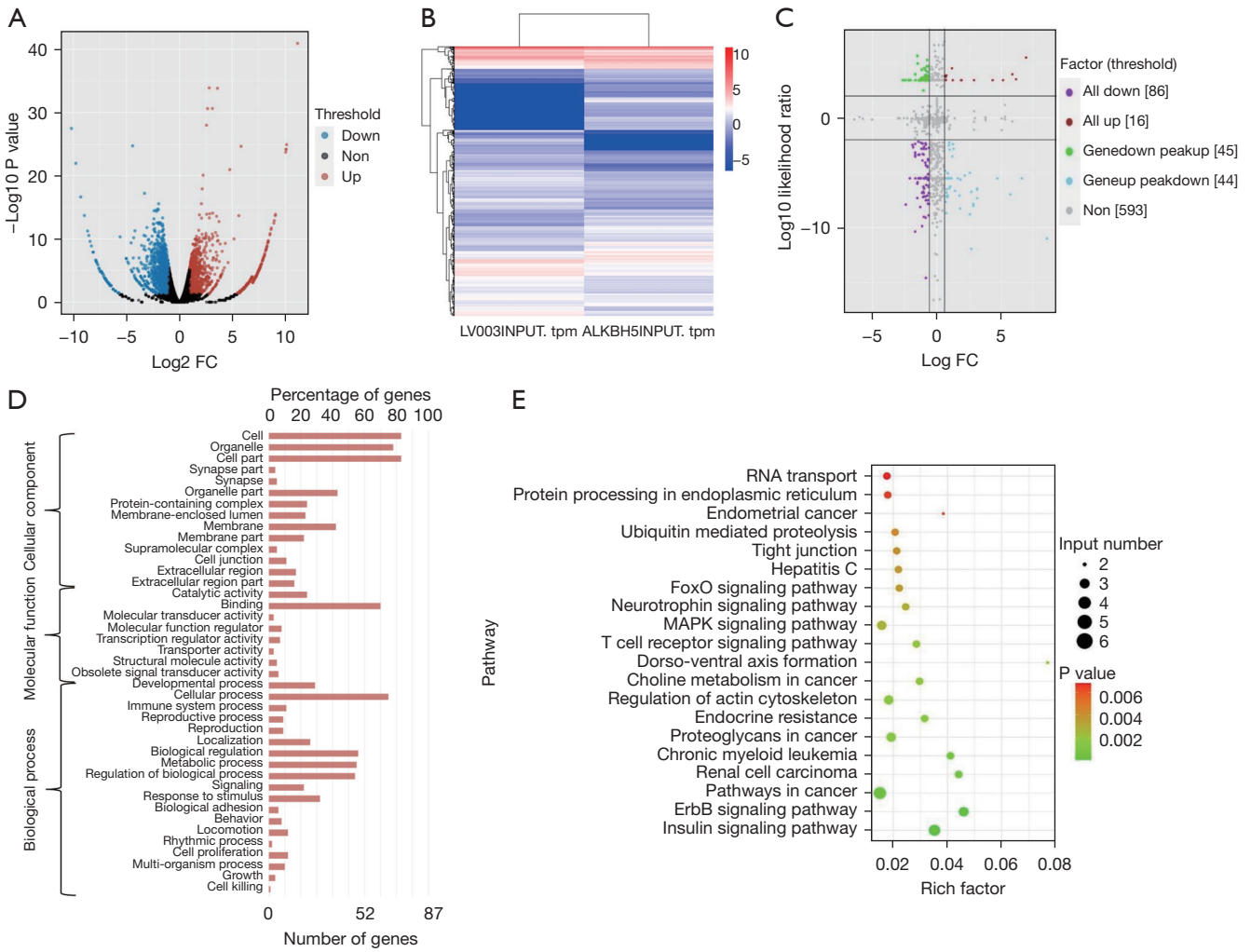

Figure 6 Identification and analysis of mRNAs with different methylation modification and expression in ALKBH5-overexpressed HL-1 cells. Volcano plot (A) and hierarchical clustering map (B) of differently expressed mRNAs in ALKBH5-overexpressed HL-1 cells (|logFC| >1, P<0.05). (C) The 9 quadrantal diagram displaying the distribution of mRNAs, which were obviously altered in m^{6}A modification and mRNA expression. GO (D) and KEGG (E) analysis of the mRNAs with significant changes in both m^{6}A modification and mRNA expression. mRNA, messenger RNA; GO, Gene Ontology; KEGG, Kyoto Encyclopedia of Genes and Genomes; FC, fold change; ALKBH5, AlkB homolog 5; m^{6}A, N^6-methyladenosine; FoxO, forkhead box O; MAPK, mitogen-activated protein kinase.

Validation of key mRNAs and methylation analysis of Trio in ALKBH5-overexpressed HL-1 cells

According to the filtered mRNAs with different methylation modifications and expressions, we further screened mRNAs with the most potential. The screening conditions included decreased m^{6}A peak, increased mRNA expression, logFC >1.1, and gene names. Initially, we confirmed 10 mRNAs including Zfp235, Hexim2, Zfp81, Map1a, Neil3, Cuedc1, Slc25a53, Trio, Msantd3, and Pnp. The results of RT-qPCR showed that Map1a, Neil3, Cuedc1, Slc25a53, Trio, Msantd3, and Pnp were markedly upregulated in the ALKBH5 group with respect to that in LV003 group (*Figure 7A*). In line with the RT-qPCR results and literature research, we further selected 3 key cardiac mRNAs (Neil3, Trio, and Pnp) that were up-regulated and related to heart for verification. The results of MeRIP-qPCR indicated that the methylation modification of Trio was notably reduced in the ALKBH5 group versus that in the LV003 group, while PNP was significantly risen (*Figure 7B*). Notably, NEIL3

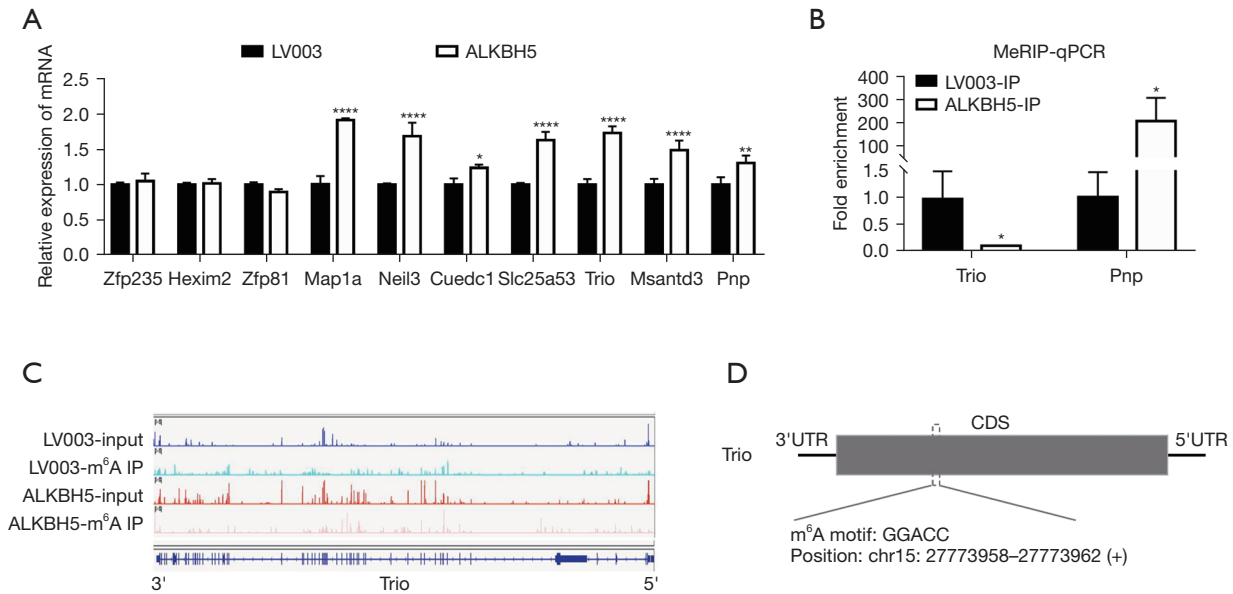

Figure 7 Validation of key mRNAs and methylation analysis of Trio in ALKBH5-overexpressed HL-1 cells. (A) RT-qPCR identified the levels of the ten screened key mRNAs in ALKBH5-overexpressed HL-1 cells. (B) MeRIP-qPCR verified the changes in the methylation levels of Neil3, Trio and Pnp. (C) m^{6}A methylated peaks for Trio was shown with Integrative Genomics Viewer (IGV) plots. (D) m^{6}A motif of Trio was exhibited. *, P<0.05; **, P<0.01; ****, P<0.0001. mRNA, messenger RNA; RT-qPCR, reverse transcription quantitative polymerase chain reaction; MeRIP-qPCR, methylated RNA immunoprecipitation quantitative polymerase chain reaction; CDS, coding sequence; ALKBH5, AlkB homolog 5; m^{6}A, N^6-methyladenosine; UTR, untranslated region.

was not detected by meRIP-qPCR. Next, Trio, which was consistent with the sequencing results, was selected for further analysis. Integrative Genomics Viewer (IGV; https://software.broadinstitute.org/software/igv/) plots displayed the distribution of m^{6}A methylated peaks for Trio (*Figure 7C*). The m^{6}A motif of Trio was GGACC, which was located in chr15: 27773958-277739^{6}2 (+) analyzed by IGV visual software (*Figure 7D*). Consequently, we demonstrated that ALKBH5 could upregulate Trio expression by reducing the methylation level of Trio.

Discussion

It is clear that MIRI is the key factor affecting the overall curative effect of cardiovascular disease and cardiac surgery (31,32). The current mechanism of MIRI is not fully elucidated, which is mainly connected with calcium overload, inflammatory response, oxidative stress, and other factors (33). These factors can result in myocardial intima damage and mitochondrial metabolism abnormalities, then accelerate ventricular remodeling, increase myocardial ischemia area, induce inflammatory injury, and eventually cause cardiac function decline or myocardial injury (33). To further investigate the latent molecular mechanisms affecting MIRI, we constructed MIRI mouse models by referencing previous research (34). The LDH and cTnI levels, infarct size, and apoptosis were increased in the MIRI mice. We showed that the m^{6}A level in total RNA was elevated in the MIRI mice, indicating the relevance between m^{6}A modification and MIRI.

Modification of m^{6}A is a high abundance epigenetic transcriptome modification in eukaryotic mRNA (35). Regulation of m^{6}A is mainly controlled by 3 regulatory factors, including methylase, demethylase, and binding protein (36). The methylation of m^{6}A RNA is mainly regulated by METTL3, METTL14, and WTAP (34), among which METTL3 is a subunit of the S-adenosyl-L-methionine (SAM) and METTL14 is a highly homologous compound of METTL3. The m^{6}A demethylase includes ALKBH5 and FTO, which belong to the ALKB family and depend on Fe^{2+} and α-ketoglutaric acid for demethylation (37). Both YTHDF1-3 and YTHDC1-2 are proteins that specifically recognize the m^{6}A site (37). Multiple studies have shown that the latent regulatory

mechanisms of m^{6}A modification are associated with a variety of cardiovascular disease (18,19). It has been reported that the m6A and METTL14 protein levels are increased in MIRI hearts and neonatal mouse cardiomyocytes upon oxidative stress (38). Increased FTO could block apoptosis of myocardial cells with hypoxia/reoxygenation through changing m^{6}A modification of Mhrt (39); WTAP could facilitate MIRI via regulating m^{6}A modification of activating transcription factor 4 (ATF4) (40); and METTL3 could weaken apoptosis of cardiomyocyte with MIRI (41). In the current study, we identified the changes in the expression of genes associated with m^{6}A modification and signified that the increased m^{6}A level was relevant to MIRI, and ALKBH5 mRNA and protein were downregulated in the MIRI mice. Existing literature has not yet elucidated the impact of ALKBH5 on MIRI. Thus, we speculated that the mechanism of m^{6}A modification alteration after MIRI might be partially regulated by ALKBH5. Subsequently, our study confirmed that the overexpression of ALKBH5 could induce proliferation, attenuate the content of LDH, apoptosis, and m^{6}A level in OGD/R-induced HL-1 cells, indicating the protective effect of ALKBH5 overexpression on MIRI. Meanwhile, we uncovered that silencing of ALKBH5 could reduce proliferation and enhance LDH content, apoptosis, and m^{6}A level in HL-1 cells, suggesting the destructive effect of ALKBH5 silencing on HL-1 cells. Thus, we demonstrated that ALKBH5 is critical in MIRI.

As a high-throughput sequencing technique integrated with immunoprecipitation, MeRIP-Seq makes it possible to study the methylation properties of m^{6}A in the whole transcriptome (42,43). Currently, MeRIP-Seq has been applied to test mRNAs mediated by m^{6}A modification in various diseases, such as glioblastoma (44), colorectal cancer (45), pancreatic cancer (46), and traumatic brain injury (47), among others. In this study, we also utilized MeRIP-Seq to analyze the underlying mRNAs related to m^{6}A methylation in ALKBH5-overexpressed HL-1 cells. Our data filtrated 503 m^{6}A peaks that had altered methylation levels including 145 m^{6}A peaks with increased methylation levels (mainly on chromosome 1, 2, and 6) and 358 m^{6}A peaks with decreased methylation levels (mainly on chromosomes 1, 2, and 9) in ALKBH5-overexpressed HL-1 cells. We also discovered 2,764 differentially expressed mRNAs (1,280 upregulated mRNAs and 1,484 downregulated mRNAs) in ALKBH5-overexpressed HL-1 cells. According to the data from MeRIP-Seq and RNA-seq, we collated a large number of mRNAs with different methylation modification and expression, which were prevailingly relevant to pathways in cancer, insulin, ErbB, and MAPK pathway in ALKBH5-overexpressed HL-1 cells. Through verification, we found that Trio with decreased m^{6}A modification was up-regulated in ALKBH5-overexpressed HL-1 cells, and the key cardiac mRNAs were relevant to the heart. The m^{6}A motif of Trio was GGACC, which is located in chr15: 27773958-277739^{6}2 (+). Trio has been reported to be associated with the MAPK pathway (48). Based on our data analysis, the MAPK pathway is the key pathway of ALKBH5 in regulating methylation modification and gene expression. Therefore, we speculated that ALKBH5 might up-regulate Trio by down-regulating the m^{6}A level of Trio and activating the MAPK pathway, thereby inducing cell proliferation. This work deserves further exploration and experimental validation *in vivo*.

Conclusions

Summarily, this study verified the protective properties of ALKBH5 on cell proliferation, cell injury, and apoptosis in the MIRI process by overexpressing or silencing it in experimental cells. Besides, we identified a mass of latent different mRNAs with m^{6}A modification variation in ALKBH5-overexpressed HL-1 cells. We further screened the most potential targeted mRNAs and suggested that Trio mRNA could be upregulated by ALKBH5 by reducing the m^{6}A level of Trio. These results may provide a basis for unearthing effective predictors and therapeutic strategies for MIRI.

Acknowledgments

Funding: This work was supported by the Maoming Science and Technology Program (No. 2020KJZX003); the High-Level Hospital Construction Research Project of Maoming People's Hospital (No. zx2020016); National Natural Science Foundation of China (82100275 to Liu NB, 81900285 to Lei LM); and the Special Project of Dengfeng Program of Guangdong Provincial People's Hospital (Nos. DFJH201812, KJ012019119, and KJ012019423).

Footnote

Reporting Checklist: The authors have completed the ARRIVE reporting checklist. Available at https://atm.amegroups.com/article/view/10.21037/atm-22-1289/rc

Data Sharing Statement: Available at https://atm.amegroups.

com/article/view/10.21037/atm-22-1289/dss

Conflicts of Interest: All authors have completed the ICMJE uniform disclosure form (available at https://atm.amegroups.com/article/view/10.21037/atm-22-1289/coif). All authors report that this work was supported by the Maoming Science and Technology Program (No. 2020KJZX003); the High-Level Hospital Construction Research Project of Maoming People's Hospital (No. zx2020016); National Natural Science Foundation of China (82100275 to Liu NB, 81900285 to Lei LM); and the Special Project of Dengfeng Program of Guangdong Provincial People's Hospital (Nos. DFJH201812, KJ012019119, and KJ012019423). The authors have no other conflicts of interest to declare.

Ethical Statement: The authors are accountable for all aspects of the work in ensuring that questions related to the accuracy or integrity of any part of the work are appropriately investigated and resolved. All animal operations were approved by the Ethics Committee of Guangdong Provincial People's Hospital (No. KY-D-2021-102-01) and conducted with the NIH guiding principles for the care and use of animals.

References

1. Reed GW, Rossi JE, Cannon CP. Acute myocardial infarction. Lancet 2017;389:197-210.
2. Toldo S, Mauro AG, Cutter Z, et al. Inflammasome, pyroptosis, and cytokines in myocardial ischemia-reperfusion injury. Am J Physiol Heart Circ Physiol 2018;315:H1553-68.
3. Shin B, Cowan DB, Emani SM, et al. Mitochondrial Transplantation in Myocardial Ischemia and Reperfusion Injury. Adv Exp Med Biol 2017;982:595-619.
4. Wang H, Chen C, Li B, et al. Nomogram to predict survival outcome of patients with veno-arterial extracorporeal membrane oxygenation after refractory cardiogenic shock. Postgrad Med 2022;134:37-46.
5. Mokhtari-Zaer A, Marefati N, Atkin SL, et al. The protective role of curcumin in myocardial ischemia-reperfusion injury. J Cell Physiol 2018;234:214-22.
6. Wu Y, Liu H, Wang X. Cardioprotection of pharmacological postconditioning on myocardial ischemia/reperfusion injury. Life Sci 2021;264:118628.
7. Rout A, Tantry US, Novakovic M, et al. Targeted pharmacotherapy for ischemia reperfusion injury in acute myocardial infarction. Expert Opin Pharmacother 2020;21:1851-65.
8. Duan B. Concise Review: Harnessing iPSC-derived Cells for Ischemic Heart Disease Treatment. J Transl Int Med 2020;8:20-5.
9. Zhang L, Lu Q, Chang C. Epigenetics in Health and Disease. Adv Exp Med Biol 2020;1253:3-55.
10. Zhang SL, Wang YQ, Zhang JH, et al. Methylated p16 gene is associated with negative expression of estrogen receptor, progesterone receptor and human epidermal growth factor receptor 2 in breast cancer. Eur J Gynaecol Oncol 2021;42:530-6.
11. Chen YG, Chen R, Ahmad S, et al. N6-Methyladenosine Modification Controls Circular RNA Immunity. Mol Cell 2019;76:96-109.e9.
12. Dai D, Wang H, Zhu L, et al. N6-methyladenosine links RNA metabolism to cancer progression. Cell Death Dis 2018;9:124.
13. Liu J, Yue Y, Han D, et al. A METTL3-METTL14 complex mediates mammalian nuclear RNA N6-adenosine methylation. Nat Chem Biol 2014;10:93-5.
14. Ping XL, Sun BF, Wang L, et al. Mammalian WTAP is a regulatory subunit of the RNA N6-methyladenosine methyltransferase. Cell Res 2014;24:177-89.
15. Yeo GS, O'Rahilly S. Uncovering the biology of FTO. Mol Metab 2012;1:32-6.
16. Zheng G, Dahl JA, Niu Y, et al. ALKBH5 is a mammalian RNA demethylase that impacts RNA metabolism and mouse fertility. Mol Cell 2013;49:18-29.
17. Zhou Z, Lv J, Yu H, et al. Mechanism of RNA modification N6-methyladenosine in human cancer. Mol Cancer 2020;19:104.
18. Qin Y, Li L, Luo E, et al. Role of m6A RNA methylation in cardiovascular disease (Review). Int J Mol Med 2020;46:1958-72.
19. Zhao K, Yang CX, Li P, et al. Epigenetic role of N6-methyladenosine (m6A) RNA methylation in the cardiovascular system. J Zhejiang Univ Sci B 2020;21:509-23.

20. Zheng N, Su J, Hu H, et al. Research Progress of N6-Methyladenosine in the Cardiovascular System. Med Sci Monit 2020;26:e921742.
21. Sessler DI, Khanna AK. Perioperative myocardial injury and the contribution of hypotension. Intensive Care Med 2018;44:811-22.
22. Yang C, Fan Z, Yang J. m6A modification of LncRNA MALAT1: A novel therapeutic target for myocardial ischemia-reperfusion injury. Int J Cardiol 2020;306:162.
23. Wu Z, Shi Y, Lu M, et al. METTL3 counteracts premature aging via m6A-dependent stabilization of MIS12 mRNA. Nucleic Acids Res 2020;48:11083-96.
24. Song H, Feng X, Zhang H, et al. METTL3 and ALKBH5 oppositely regulate m6A modification of TFEB mRNA, which dictates the fate of hypoxia/reoxygenation-treated cardiomyocytes. Autophagy 2019;15:1419-37.
25. Han Z, Wang X, Xu Z, et al. ALKBH5 regulates cardiomyocyte proliferation and heart regeneration by demethylating the mRNA of YTHDF1. Theranostics 2021;11:3000-16.
26. Peng YJ, He WQ, Tang J, et al. Trio is a key guanine nucleotide exchange factor coordinating regulation of the migration and morphogenesis of granule cells in the developing cerebellum. J Biol Chem 2010;285:24834-44.
27. Xu Z, Alloush J, Beck E, et al. A murine model of myocardial ischemia-reperfusion injury through ligation of the left anterior descending artery. J Vis Exp 2014;(86):51329.
28. Chen Y, Zhao Y, Chen J, et al. ALKBH5 suppresses malignancy of hepatocellular carcinoma via m6A-guided epigenetic inhibition of LYPD1. Mol Cancer 2020;19:123.
29. The Gene Ontology Consortium. Expansion of the Gene Ontology knowledgebase and resources. Nucleic Acids Res 2017;45:D331-8.
30. Kanehisa M, Furumichi M, Tanabe M, et al. KEGG: new perspectives on genomes, pathways, diseases and drugs. Nucleic Acids Res 2017;45:D353-61.
31. Yuan L, Dai X, Fu H, et al. Vaspin protects rats against myocardial ischemia/reperfusion injury (MIRI) through the TLR4/NF-κB signaling pathway. Eur J Pharmacol 2018;835:132-9.
32. Zheng Y, Chen S, Yang Y, et al. Uncovering the molecular mechanisms of Ilex pubescens against myocardial ischemia-reperfusion injury using network pharmacology analysis and experimental pharmacology. J Ethnopharmacol 2022;282:114611.
33. Li L, Li X, Zhang Z, et al. Protective Mechanism and Clinical Application of Hydrogen in Myocardial Ischemia-reperfusion Injury. Pak J Biol Sci 2020;23:103-12.
34. Li Y, Fei L, Wang J, et al. Inhibition of miR-217 Protects Against Myocardial Ischemia-Reperfusion Injury Through Inactivating NF-κB and MAPK Pathways. Cardiovasc Eng Technol 2020;11:219-27.
35. Erson-Bensan AE, Begik O. m6A Modification and Implications for microRNAs. Microrna 2017;6:97-101.
36. Liu ZX, Li LM, Sun HL, et al. Link Between m6A Modification and Cancers. Front Bioeng Biotechnol 2018;6:89.
37. Luo Q, Gao Y, Zhang L, et al. Decreased ALKBH5, FTO, and YTHDF2 in Peripheral Blood Are as Risk Factors for Rheumatoid Arthritis. Biomed Res Int 2020;2020:5735279.
38. Pang P, Qu Z, Yu S, et al. Mettl14 Attenuates Cardiac Ischemia/Reperfusion Injury by Regulating Wnt1/β-Catenin Signaling Pathway. Front Cell Dev Biol 2021;9:762853.
39. Shen W, Li H, Su H, et al. FTO overexpression inhibits apoptosis of hypoxia/reoxygenation-treated myocardial cells by regulating m6A modification of Mhrt. Mol Cell Biochem 2021;476:2171-9.
40. Wang J, Zhang J, Ma Y, et al. WTAP promotes myocardial ischemia/reperfusion injury by increasing endoplasmic reticulum stress via regulating m6A modification of ATF4 mRNA. Aging (Albany NY) 2021;13:11135-49.
41. Zhao X, Yang L, Qin L. Methyltransferase-like 3 (METTL3) attenuates cardiomyocyte apoptosis with myocardial ischemia-reperfusion (I/R) injury through miR-25-3p and miR-873-5p. Cell Biol Int 2021. [Epub ahead of print].
42. Meng J, Lu Z, Liu H, et al. A protocol for RNA methylation differential analysis with MeRIP-Seq data and exomePeak R/Bioconductor package. Methods 2014;69:274-81.
43. Zhang Y, Hamada M. MoAIMS: efficient software for detection of enriched regions of MeRIP-Seq. BMC Bioinformatics 2020;21:103.
44. Li F, Yi Y, Miao Y, et al. N6-Methyladenosine Modulates Nonsense-Mediated mRNA Decay in Human Glioblastoma. Cancer Res 2019;79:5785-98.
45. Chen X, Xu M, Xu X, et al. METTL14-mediated N6-methyladenosine modification of SOX4 mRNA inhibits tumor metastasis in colorectal cancer. Mol Cancer 2020;19:106.
46. Wang M, Liu J, Zhao Y, et al. Upregulation of METTL14 mediates the elevation of PERP mRNA N6 adenosine methylation promoting the growth and metastasis of pancreatic cancer. Mol Cancer 2020;19:130.

47. Yu J, Zhang Y, Ma H, et al. Epitranscriptomic profiling of N6-methyladenosine-related RNA methylation in rat cerebral cortex following traumatic brain injury. Mol Brain 2020;13:11.
48. Chen H, Guo S, Xia Y, et al. The role of Rho-GEF Trio in regulating tooth root development through the p38 MAPK pathway. Exp Cell Res 2018;372:158-67.

(English Language Editor: J. Jones)

Cite this article as: Li J, Chen J, Zhao M, Li Z, Liu N, Fang H, Fang M, Zhu P, Lei L, Chen C. Downregulated ALKBH5 contributes to myocardial ischemia/reperfusion injury by increasing m^{6}A modification of Trio mRNA. Ann Transl Med 2022;10(7):417. doi: 10.21037/atm-22-1289

